SKBF TECHNICAL REPORT
KBS
83-72

On the thermal conductivity and thermal diffusivity of highly compacted bentonite

Sven Knutsson
University of Luleå

Luleå, Sweden October 1983

SVENSK KÄRNBRÄNSLEFÖRSÖRJNING AB / AVDELNING KBS
Swedish Nuclear Fuel Supply Co/Division KBS
MAILING ADDRESS: SKBF/KBS, Box 5864, S-102 48 Stockholm, Sweden
Telephone 08-67 95 40

ON THE THERMAL CONDUCTIVITY AND THERMAL DIFFUSIVITY OF HIGHLY COMPACTED BENTONITE

Sven Knutsson

Division of Soil Mechanics
University of Luleå
Luleå, Sweden October 1983

A list of other reports published in this series during 1983 is attached at the end of this report. Information on KBS technical reports from 1977-1978 (TR 121), 1979 (TR 79-28), 1980 (TR 80-26), 1981 (TR 81-17) and 1982 (TR 82-28) is available through SKBF/KBS.

SUMMARY

The report concerns the thermal conductivity and the thermal diffusivity of highly compacted bentonite, which has been suggested as embedding substance in the Swedish concept for the disposition of highly radioactive unreprocessed nuclear waste products.

The first part of the report describes the testing method used, which is called the Transient Hot Strip method (THS). By this, the thermal conductivity and the thermal diffusivity were determined simultaneously in a test which was performed within 10-15 seconds. The measuring unit was a small metal strip, which was placed in the center of the tested bentonite sample. Due to the short measuring time (10-15 sec), the risk of water redistribution due to thermal gradients was reduced to a minimum. This made the method well adapted for the determination of the thermal properties of the moist bentonite.

The experimental set-up, including the use of the swelling pressure oedometers in which the bentonite samples were mounted, with the metal strip in the center, are described.

The second part of the report, describes the experiments, which were performed on bentonite bodies, mostly cylindrical in shape with a diameter of 50 mm and a height of 20 mm.

From the tests of the air dry samples it was found that the thermal conductivity increased as the pressure on the sample increased. This was explained by an improved thermal contact between the measuring metal strip and the bentonite body at increasing pressure. The determined conductivities were compared with the values obtained from a theoretical model for the

prediction of the thermal conductivity of moist geological materials. The agreement was good and the model was then used to calculate the thermal conductivity of the bentonite as water was taken up by the sample. The experimentally obtained conductivities during this process, agreed fairly well with the calculated values.

At low pressures, the thermal conductivity was found to be 0.83-1.08 W/m,K at a water content of 4.1% and a bulk density of 1.96-2.17 t/m^3. At complete water saturation, the conductivity was estimated at 1.35--1.45 W/m,K at the bulk density of 2.0-2.1 t/m^3, being representative for the ultimate conditions in a repository.

The mass heat capacity of the bentonite was found to be 0.96-1.05 J/g,K, which was slightly higher than the expected value that can be derived on values from the literature. The successfully increasing volumetric heat capacity during water uptake was also determined and this was predicted by the model used.

On the thermal conductivity and thermal diffusivity of highly compacted bentonite

Sven Knutsson
Div of Soil Mechanics
University of Luleå

October 1983

CONTENTS

1. INTRODUCTION

The Swedish concept for the disposition of highly radioactive, unreprocessed nuclear waste products implies that copper canisters containing the radioactive material be surrounded by highly compacted Na bentonite clay. In the repository the dense clay separates the canisters from the rock and the thermal properties of the clay is therefore of major concern.

The thermal conductivity of the buffer substance is the main parameter since it controls how effectively the heat produced in the canister is transported through the clay to the rock. If an accurate calculation of the time dependent temperature field around a canister is to be performed, information of the volumetric heat capacity of the buffer substance is needed as well.

In a porous mass the porosity as well as the water content have a major influence on the thermal properties in addition to the conductivity and heat capacity of the solid phase itself. It is therefore of great importance to know how the properties change as water is taken up as well as the rate of this process.

During the initial phase of deposition, the buffer substance of bentonite will have a moderate water content of 8 -13%. When the repository is closed water migrates from the rock into the clay in which the water content increases. This yields successively higher values of the thermal parameters thus implying decreasing temperatures in the vicinity of the canister. This means that the initial stage of deposition will be the least

favourable; i.e. a low water content and thus low thermal conductivity and the highest temperatures.

The scope of this study has been to determine the thermal conductivity and the thermal diffusivity of highly compacted bentonite when water is taken up and the water content increases.

A second purpose has been to compare theoretically computed values of the thermal properties and experimentally determined equivalents.

2. MATERIAL

All the tests in this study have been performed on samples of highly compacted bentonite. The clay material consisted of granulated Na bentonite type MX-80 (American Colloid Co). The granulometric composition was characterized by a minus 2 μm content of approximately 85% and a montmorillonite content of about 80-90% of this fraction [5].

From the air-dry material high density clay bodies were made by compressing the powder under high pressure (50 MPa). The procedure yielded almost homogeneous bodies with preset densities. Most test samples had a cylindrical shape with a diameter of 50 mm and a height of 10 mm, while some were rectangular. These were made by cutting big blocks of compacted bentonite into pieces of desired shape.

The initial water content of the samples varied between 4% and 14% and the bulk densities were of the order 1,96-2,17 t/m^3.

3. TESTING METHOD

The testing method used for the determination of the thermal properties (the thermal conductivity and the volumetric heat capacity), is a newly developed technique called Transient Hot Strip method (THS). It was developed at the Department of Physics at the Chalmers University of Technology and is described in detail in [1] and [2]. The main advantages of the THS-method compared to other techniques are:

1. The measuring procedure is very fast, each test is performed within 10-15 seconds. This reduces the risk of water redistribution due to thermal gradients to a minimum. This is of special concern, when tests are made on moist samples.

2. The test is developed for simultaneous measurement of the thermal conductivity (λ) and the thermal diffusivity (a), i.e. the quotient between thermal conductivity and volumetric heat capacity.

3. The temperature increase in the measuring unit is small, below 0,5 K. This reduces the temperature gradients in the sample to low values.

4. The measuring unit consists of a thin metal strip with small dimensions. This makes it possible to measure the thermal properties of small objects.

3.1 Testing principle

The testing principle, as well as the exact mathematical deductions are given in detail in [2]. In this report just a brief description of the testing technique will be given.

A very thin metal film is brought in contact with the investigated material. The metal film is then used as a plane heat source and as a resistance thermometer. When testing solid material the metal strip is pressed between two pieces of the material. The two pieces must have at least one flat surface each, so the metal strip is approximately a plane heat source. During the test, a constant electrical current is supplied to the metal film. Thus, heat is produced according to the electrical resistance in the strip and consequently its temperature increases. This causes an increasing electrical resistance of the strip, since this is dependant of the temperature. This is monitored as a subsequent voltage increase between the two ends of the strip.

The temperature increase of the metal strip is due to how fast the heat is conducted into the surrounding material. If this has a high thermal conductivity, heat is carried away quickly, yielding a low temperature increase and thus a low value of the monitored change of the electrical voltage. On the contrary, if the thermal conductivity has a low value the temperature of the metal strip is increased to higher values giving rise to large changes of the monitored voltage change. Consequently, the change of the electrical voltage between the two ends of the metal strip, can be directly related to the thermal properties of the material surrounding the strip.

The electrical current is supplied to the metal strip during 5 to 10 seconds and the voltage between its ends (U_t) is simultaneously recorded by a digital voltmeter. The data recorded is directly transmitted to a computer where all the calculations are performed. The thermal conductivity and diffusivity are thus measured within a very short time. It is of course required, that the electrical current, the resistivity and the dimensions of the metal film are all known with sufficient accuracy.

The electrical resistivity of the metal strip changes with the time after the onset of the heating, according to equation (1)

$$\rho(T) = \rho_o[1+\alpha(T(0,y,t)-T_o)] \qquad (1)$$

where

ρ_o is the resistivity of the metal strip at the temperature T_o, i.e. before the test

$\rho(T)$ is the resistivity at the temperature T

α is the temperature dependence of the resistivity of the metal used for the strip

$T(0,y,t)$ is the temperature at the surface of the metal strip at the position y at the time t

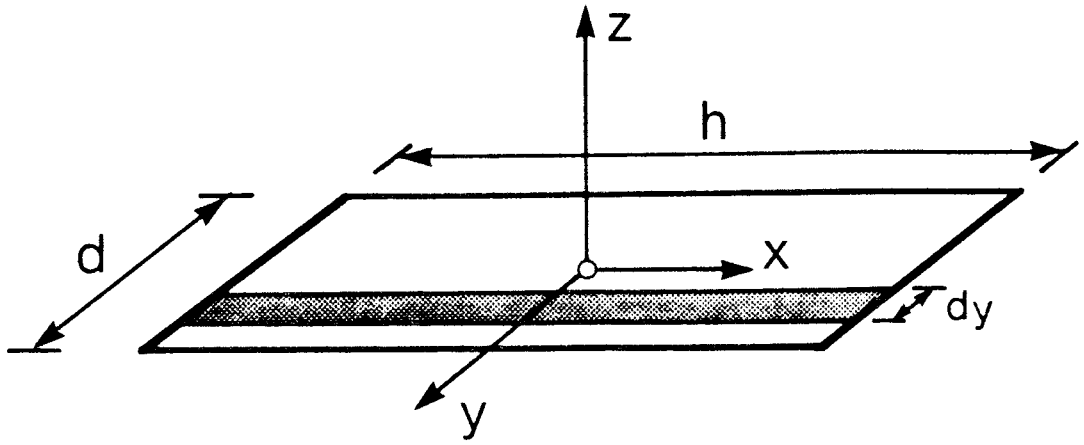

Fig. 3.1 The metal strip with the coordinate system used for the mathematical deductions

Since the resistance of an element of the strip is given by eq. (2), the total resistance of the strip can be expressed by (3)

$$dR(T) = \rho(T)h/\nu dy \tag{2}$$

where

h is the total length of the strip
ν is the thickness of the strip

$$R(t) = R_o \left[1 + \frac{\alpha}{d} \int_{-\frac{d}{2}}^{\frac{d}{2}} (T(0,y,t) - T_o)dy\right] \tag{3}$$

$$R_o = \frac{\rho(T_o) \cdot h}{\nu d} \tag{4}$$

$R(t)$ is the total resistance of the metal strip at the time (t) after the onset of the current

The integral divided by the width (d) in equation (3), can be regarded as an average temperature rise in the strip at time t (ΔT_t). It should be noticed, however, that equation (3) is valid only if the value of α is small and the temperature increase of the strip is restricted to low values. A typical maximum increase is 0,5 K. From [2] it is concluded, that α can be regarded as sufficiently small if it is smaller than $5 \cdot 10^{-3} K^{-1}$.

By using Ohm's law, with a constant current through the strip (I) the voltage between the two ends of the strip is now given by eq. (5)

$$U(t) = U_o(1 + \alpha \Delta T_t) \qquad (5)$$

where

U_o is the initial voltage at time t=0

By solving the differential equation of heat conduction, with appropriate boundary and initial conditions, a value of ΔT_t can be obtained. Analytical solutions for many problems are given in [3], from which the present solution was derived.

By introducing ΔT_t in equation (5), the final expression for the total variation of the electrical voltage between the two ends of the metal strip yields eq. (6).

$$U(t) = U_o \left[1 + \frac{\alpha I U_o}{2h\lambda\sqrt{\pi}} \; f\,(B\sqrt{t}) \right] \tag{6}$$

$$B = \frac{2\sqrt{a}}{d} \tag{7}$$

where

a = thermal diffusivity
h = the length of the metal strip
d = the width of the strip

The function $f(B\sqrt{t})$ can be computed for given values of B and t according to (8)

$$f(B\sqrt{t}) = B\sqrt{t}\ \mathrm{erf}\left(\frac{1}{B\sqrt{t}}\right) - \frac{B^2 t}{\sqrt{4\pi}}\left[1 - \exp\left(\frac{-1}{B^2 t}\right)\right] +$$

$$+ \frac{1}{\sqrt{4\pi}}\left[-\mathrm{Ei}\left(\frac{-1}{B^2 t}\right)\right] \tag{8}$$

in eq. (8)

$$\mathrm{erf}(z) = \frac{2}{\sqrt{\pi}} \int_o^z e^{-x^2} dx \tag{9}$$

$$\mathrm{Ei}(-z) = -\int_z^\infty x^{-1} \exp(-x)\, dx \tag{10}$$

Eq.(6) can be put in the form of eq.(11)

$$U_t = U_o + C\, f(B\sqrt{t}) \tag{11}$$

in which

$$C = \frac{\alpha I U_o^2}{2h\lambda\sqrt{\pi}} \tag{12}$$

The meaning of eq. (11) is, that for the right value of the factor B there will be a linear relationship between the voltage U_t and the function $f(B\sqrt{t})$.

In a test, where successive readings of the voltage (U_t) are recorded at different times (t), it is possible to find the right value of B by using an iteration procedure. The constant value of B is thus changed until the correlation coefficient as calculated from U_t and $f(B\sqrt{t})$ has reached its maximum. From this value of B it is possible to determine the thermal diffusivity by using eq. (7). The thermal conductivity is given by eq. (12), i.e. the slope and the intercept of the line with the highest correlation coefficient, since all the other parameters are known.

It should be noticed, that a main requirement for getting the two thermal properties out of one and the same test is that the metal strip has a finite width.

If this is very large, there will be a thermal gradient just in one direction and consequently the test yields information of the thermal conductivity only. On the other hand, if the strip is very narrow, approximating a very thin wire, again we will have a thermal gradient in just one direction. The latter condition has been widely used in various methods based on transient heat flow, for the determination of the thermal conductivity. Two well-known methods based on the assumption of one thermal gradient only, are the heating wire technique used in [4] and the thermal probe method.

3.2 Experimental procedure

The experimental layout of the electrical circuit was designed at the Department of Physics at Chalmers University and it is described in detail in [3]. In Fig. 3.2 the circuit is schematically illustrated. The main components are: S - the sample with its metal strip, P - the power supply, R_s - standard resistor used for the measurement of the electrical current, R - current limiting resistor and R_b - balancing resistor.

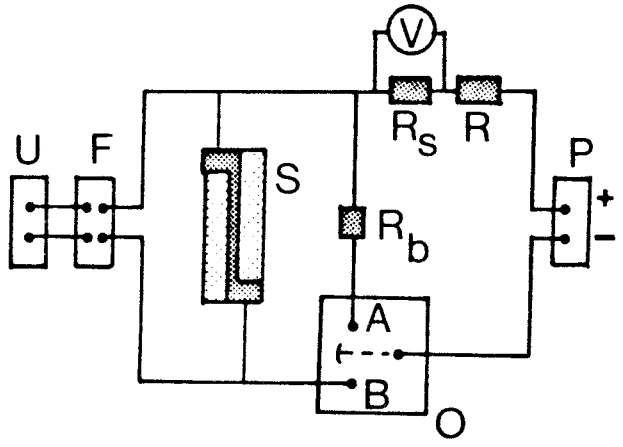

Fig. 3.2 Layout of the electrical circuit used for the THS-tests.

The resistor R has a resistance about 100 times larger than that of the metal strip. When the latter is changed during the test, no corresponding change of the current will take place, since the total resistance in the measuring circuit will be unchanged due to the high constant resistance of R.

U and V are both digital voltmeters, V being used for measuring the current and U for the detection of the voltage change in the metal strip. Since the changes are very small (10^{-4} to 10^{-6}V) a differential amplifier with an offset voltage is used in order to get as high precision as possible in the measurements. The digital voltmeter V is directly connected to a computer (HP 9825A). By this, the recording procedure is controlled and the recorded data is stored.

The recorded values of U_t is then combined with different values of the function $f(B\sqrt{t})$ until the highest coefficient of correlation is reached. From the slope and the intercept of the straight line thus obtained the thermal conductivity and the thermal diffusivity is calculated.

The small dimensions of the metal strip has made it possible to perform the measurements of the thermal properties of the bentonite, confined in a swelling pressure oedometer. The strip, having a length of 40 mm and a width of 3 mm has been placed between two halves of precompacted bentonite, which were then applied in a swelling pressure oedometer before the start of the test, see Fig. 3.3. Much effort was put to the arrangement of a leak-free passage for the electrical connections to the metal strip, because no leakage of water or clay particles from the bentonite sample was accepted. This would have had caused changes in the swelling pressure in the bentonite.

During the test, water was let in from above only, since the inlet at the lower end of the oedometer was used for the electrical connections. The determination of the swelling pressure, which was made parallel to the recording of the thermal properties, followed the same procedure as described in [5], i.e. the sample was confined in the cylindrical space and the total volume was kept constant throughout the test.

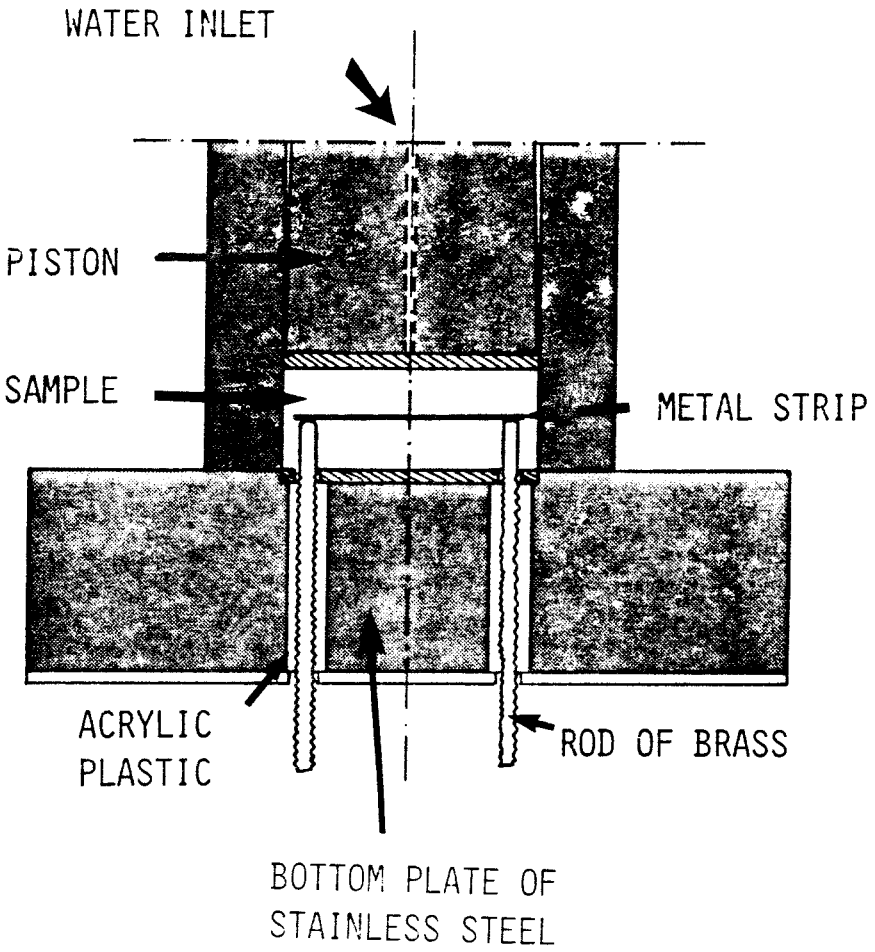

Fig. 3.3 The swelling pressure oedometer with the metal strip in the centre of the bentonite body. The arrangement for the lead-through of the electrical connectors are shown as well.

The tested bentonite samples had a diameter of 50 mm and a height of 20 mm.

As shown in Fig. 3.3 the electrical connections to the metal strip consisted of two rods of brass which were screwed through plugs of acrylic plastic glued to the bottom plate of stainless steel. This yielded a perfect sealing against leakage of water and the two rods also supplied good supports for the metal strip which was soldered to the rods.

4. TEST RESULTS

A large number of tests have been performed in order to study the variation of the thermal conductivity and the thermal diffusivity of the highly compacted bentonite (MX-80), when the densities and water contents were varied.

The experimental technique used in this work had the advantage of being fast in operation once the test equipment had been set up. This made it possible to make several test within a restricted period of time, yielding a statistical mean value and coefficient of variation for the determined thermal properties at each testing condition. Thus, each value of the thermal conductivity and diffusivity reported here, is a mean of 4 to 10 individual measurements.

Most of the tests were carried out with the bentonite samples constrained in the swelling pressure oedometers.

However, four complementary tests were carried out on non-constrained blocks of precompressed bentonite. For each test, two blocks were used being 0,08x0,04x0,015 m^3 in size. The blocks were pressed together during the test by the use of screw clamps, with the measuring metal strip in between.

The results from these tests are given in Table 1 in which the thermal conductivities ($\bar{\lambda}$) and the thermal diffusivities ($\bar{a}$) are calculated mean values. For each test the coefficients of variation (S_λ and S_a) are given as well, i.e. the ratio of the standard deviation and arithmetic mean values.

From the obtained thermal conductivity and thermal diffusivity, the volumetric heat capacity can be calculated by using eq (13).

$$\lambda = a \cdot C \qquad (13)$$

where

C = volumetric heat capacity ($J/m^3,K$)

a = thermal diffusivity (m^2/s)

Table 1. Thermal properties of highly compacted bentonite (non-constrained samples)

Test	ρ (t/m^3)	w (%)	$\bar{\lambda}$ (W/m,K)	$\bar{a}$ (10^{-7} m^2/s)	C (10^6 $J/m^3,K$)	S_λ (%)	S_a (%)
A	2,17	11,0	1,012	4,075	2,483	0,52	2,7
B	2,12	13,9	1,145	4,281	2,687	0,32	3,2
C	2,11	12,1	1,081	4,250	2,541	0,26	1,6
D	2,11	9,5	1,052	4,151	2,534	0,50	2,1

From Table 1 it is clear that the uncertainty in the determination of the thermal diffusivity is larger ($S_a \sim 2\%$) than that of the thermal conductivity ($S_\lambda < 0,5\%$). The reason for this is the experimental procedure, which is known to give the smallest variation of the thermal conductivity, see [2]. This is due to the fact that the slope of the curve $U_t = U_o + C\ f(B\sqrt{t})$ is used in this case, while the diffusivity is calculated from the factor B in eq. (7). This yields the somewhat larger variation for the latter parameter.

The highly compacted bentonite mounted in the swelling pressure oedometers had an initial water content of 4.2% in four of the tests. This is a low value but it was chosen in order to get a clear picture of the change of the thermal conductivity when water was let into the sample. The bulk densities were different in the four tests, the major characteristics being shown in Table 2.

Table 2

Sample	ρ (t/m^3)	w (%)	Porosity n (%)
1	1,97	4,2	28,7
2	1,96	4,2	29,0
3	2,09	4,2	24,3
4	2,17	4,1	21,3

When water is let into the oedometer, it is taken up by the bentonite and consequently the water content increases. At the same time a swelling pressure will develop. It is reasonable to believe that these two effects will increase the recorded thermal conductivity of the bentonite. The increasing water content will increase the thermal conductivity since water has a higher thermal conductivity than the successively replaced pore air. The swelling pressure will increase the recorded thermal conductivity, mainly by the following three effects:

- a successively better thermal contact will develop between the measuring unit, i.e. the metal strip, and the surrounding bentonite blocks when the pressure is increased. Consequently, the evaluated conductivity is increased too.

- small cracks within the precompressed blocks will be closed, when the pressure is increased. Thus a higher thermal conductivity will be obtained.

- The bentonite blocks are made of a granulated powder and the contacts between the individual granules might also be better as the pressure increases. Consequently, the thermal conductivity of the block increases.

In order to quantify the pressure dependent part of the increase of the thermal conductivity, this was determined at a successively increased pressure. The tests were made on samples 1-4, after mounting them in the oedometers but before water was let in. The pressure was externally applied to the samples by putting the oedometers in a compression machine, in which the force could be regulated with high precision. When a given pressure was reached measurements of the thermal conductivity and diffusivity were performed. The detailed tests results, as well as the coefficients of variation in each test, are given in Appendix 1. Fig. 4.1 shows the evaluated mean values of the thermal conductivity as a function of the external pressure.

In all the four samples, there is an obvious tendency of a higher value of thermal conductivity (λ) when the pressure is increased. The increase of the conductivity is 0,18 - 0,28 W/m,K as the pressure is raised from 0 to 50 MPa. The lower value (0,18) is obtained from sample 4, while sample 1 and 2 have the higher value. Sample 3 has an intermediate increase of 0,22 W/m,K.

After the pressure had been increased to 50 MPa, it was lowered stepwise to zero again. During this operation the thermal conductivity and diffusivity, were determined at the same pressures as during the pressure increasing cycle. Again, practically the same values were obtained, which indicates that no hysteresis is present. This also indicates, that no permanent structural change has taken place, since it probably should have caused a permanent change of the conductivity. Consequently, the increase of the conductivity has a temporary character mainly caused by an improved thermal contact between the metal strip and the surrounding bentonite. To some extent the closure and re-opening of microcracks can have

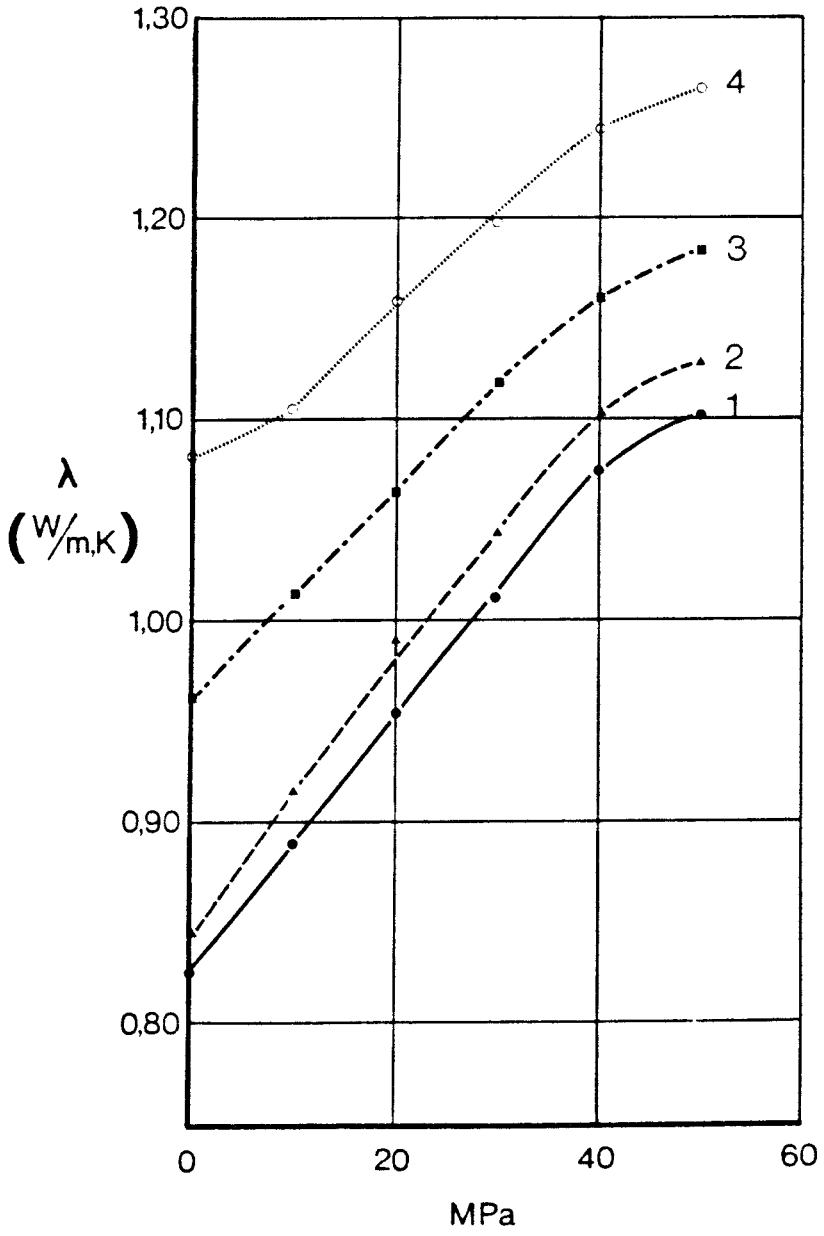

Fig. 4.1 The evaluated thermal conductivity of highly compacted bentonite for different external pressures. The tests are made before water is let into the oedometers.

had the same effect. However, these two effects cannot be separated from each other in the present study.

As can be seen in Appendix 1, the coefficient of variation of the thermal conductivity tests was very low <1%. In most of them this coefficient was actually lower than 0.6%. In the determination of the thermal diffusivity a larger scatter was found between the individual measurements in each test. Here, the coefficient of variation was found to be lower than 5%; typically about 2%, which again is higher than that for the conductivity, cf. test A - D in Table 1.

In Fig. 4.2 the thermal conductivity obtained for sample 1-4 have been replotted as a function of the bulk density. The vertical line for each sample, indicates the variation of the thermal conductivity as the pressure is changed. The lower end of the line gives the thermal conductivity at the pressure 0 MPa, while the upper end gives the value obtained for 50 MPa.

As shown in Fig. 4.2 the thermal conductivity increases with the bulk density for a constant water content. This is what could be expected, since both the dry density and the degree of water saturation are higher for sample 4 than for those with lower densities. In addition two curves A and B are shown in Fig. 4.2, curve A illustrating the thermal conductivities which can be calculated by the use of the mathematical model presented in [6] and [7]. This model gives the thermal conductivity of a non-saturated soil sample by the use of eq. (14)-(17)

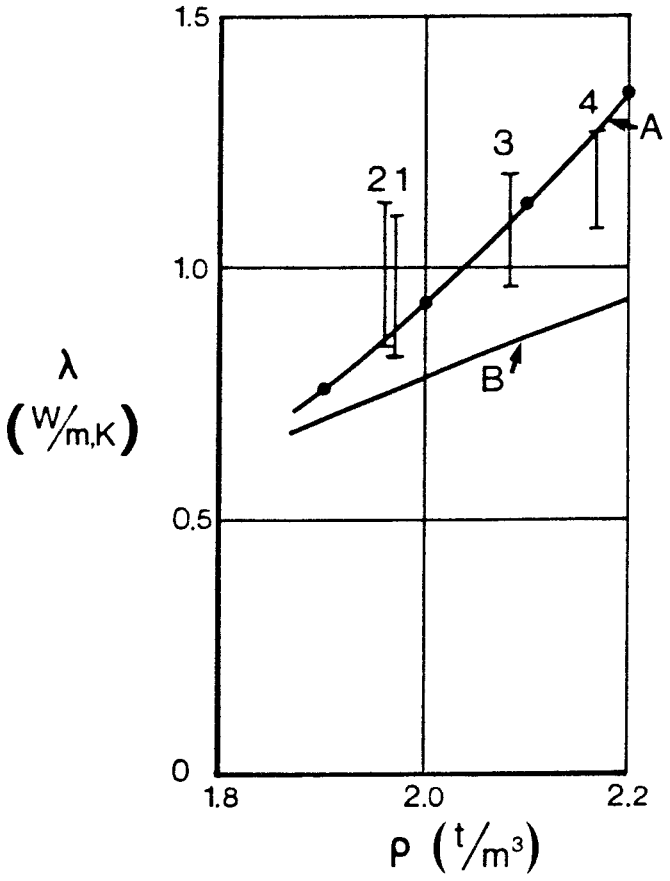

Fig. 4.2 Thermal conductivities of highly compacted bentonite with a water content of 4,2%. The vertical lines indicates the dependency of the external pressure.

$$\lambda = \lambda_o + K_e(\lambda_1 - \lambda_o) \quad (14)$$

and

$$\lambda_o = 0{,}034\ n^{-2{,}1} \quad (15)$$

$$\lambda_1 = 0{,}56^n \cdot 2^{1-n} \quad (16)$$

$$K_e = 1 + \log S_r \quad (17)$$

where

n = porosity
S_r = degree of water saturation

Eq. (15) gives the conductivity of a completely dry material, while (16) gives the corresponding value for a water saturated sample. Fig. 4.2 shows that the model yields acceptable predictions of the conductivity for compacted bentonite with low degrees of water saturation, but it has a tendency to overestimate the conductivity at higher values of the bulk density.

Another model, presented in [4] is used in comparison. and the values given by this, are shown by curve B in Fig. 4.2. However, this model underestimates the experimentally obtained values systematically by about 25 percent.

From the thermal conductivity and diffusivity obtained from the tests with different external pressure on the bentonite body, the volumetric heat capacity can be derived by using eq. (13). This value if of course highly influenced of the water content and the density of the sample and therefore it is practical to deal with the values of the specific heat, i.e. the mass heat capacity of each component. Eq. (18) gives the relationship between the volumetric (C) and mass (c_s) heat capacities with respect to the water content.

$$C = \frac{\rho}{1+w} (c_s + c_w \cdot w) \qquad (18)$$

where c_w = mass heat capacity of water (4,2 J/g,K)
w = water content
ρ = bulk density

The evaluated data of the mass heat capacities are given in detail in Appendix 1. In Fig. 4.3 the heat capacities are plotted as a function of the applied pressure.

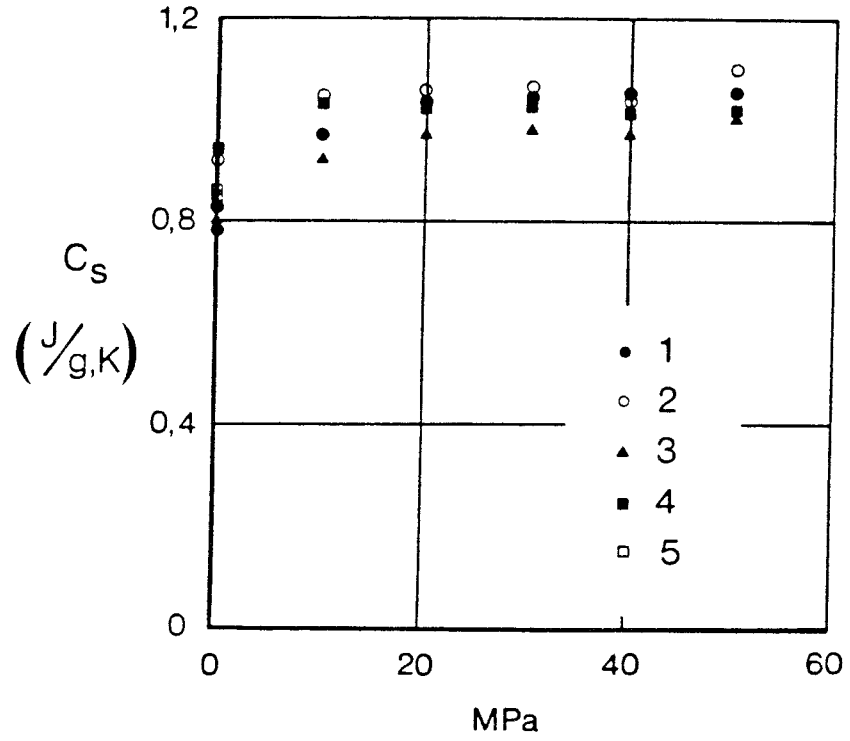

Fig. 4.3 The mass heat capacity (c_s) of highly compacted bentonite at different pressures.

At zero external pressure, the mean value of all the tests performed is 0,86 J/g,K. This is in accordance with data reported elsewhere for clays and clay-shales, i.e. 0,81-0,87 J/g,K, see [7] and [8]. However, the heat capacity seems to be pressure-dependent and at higher pressures it increases to about 1,04 J/g,K. This value is reached at 20 MPa and for pressures exceeding this, no change can be detected.

After the initial tests at the low water contents in the samples, water was let into the oedometers through the upper pistons. This made it possible for the bentonite samples to take up water, thus yielding successively larger degree of water saturation. During this process a swelling pressure was developed since the samples were totally constrained. However, during this process small internal displacements took place within the bentonite body, although the overall volume was practically kept constant. The movements were caused by the homogenizing process that ultimately leads to complete water saturation. However, small displacements caused serious damage in the experimental set up, since the metal strips mounted in the center of the samples were very fragile. Consequently, most of the metal strips were broken and thus no measurements of the thermal properties could be carried out when the water content was increasing.

Only one test out of the total number of 12 could be successfully completed. Two additional tests could be pursued during a short period of time, while the rest of the tests were unsuccessful for the reason described.

In the successful test (sample 4), the increase of the thermal conductivity as water was taken up, could be followed for about 13 days (305 hours) before the metal strip was broken. The results are shown in Fig. 4.4 as well as in Appendix 2.

As shown in Fig. 4.4 the conductivity increased from the initial value of 1,08 W/m,K for the "dry" sample (W_o=4,1%) to the final value of 1,59 W/m,K. This value was reached after about 250 hours at which time the sample was almost completely saturated.

By using eq. (16) the conductivity of the water saturated sample is found to be 1.55 W/m,K, i.e. a difference of about 0,04 W/m,K between the recorded and calculated values which corresponds to a deviation of 2,5% of the measured value.

A theoretical prediction of the successive increase of the conductivity in the bentonite has been carried out for comparison with the experimentally obtained values. The calculations were based on the assumption that the water migrated into the bentonite in the form of a diffusion process with the diffusion coefficient $4 \cdot 10^{-10}$ m^2/s, [9]. The upper boundary condition was a constant water content, corresponding to a complete water saturation in this sample; no 4, W_s=10,2%. At the bottom of the sample a condition corresponding to a free boundary was used. The latter was utilized since no flow of water could take place perpendicular to this lower end of the sample.

The increase of the water content in the center of the sample, i.e. where the metal strip was placed, was then determined by solving the diffusion equation.

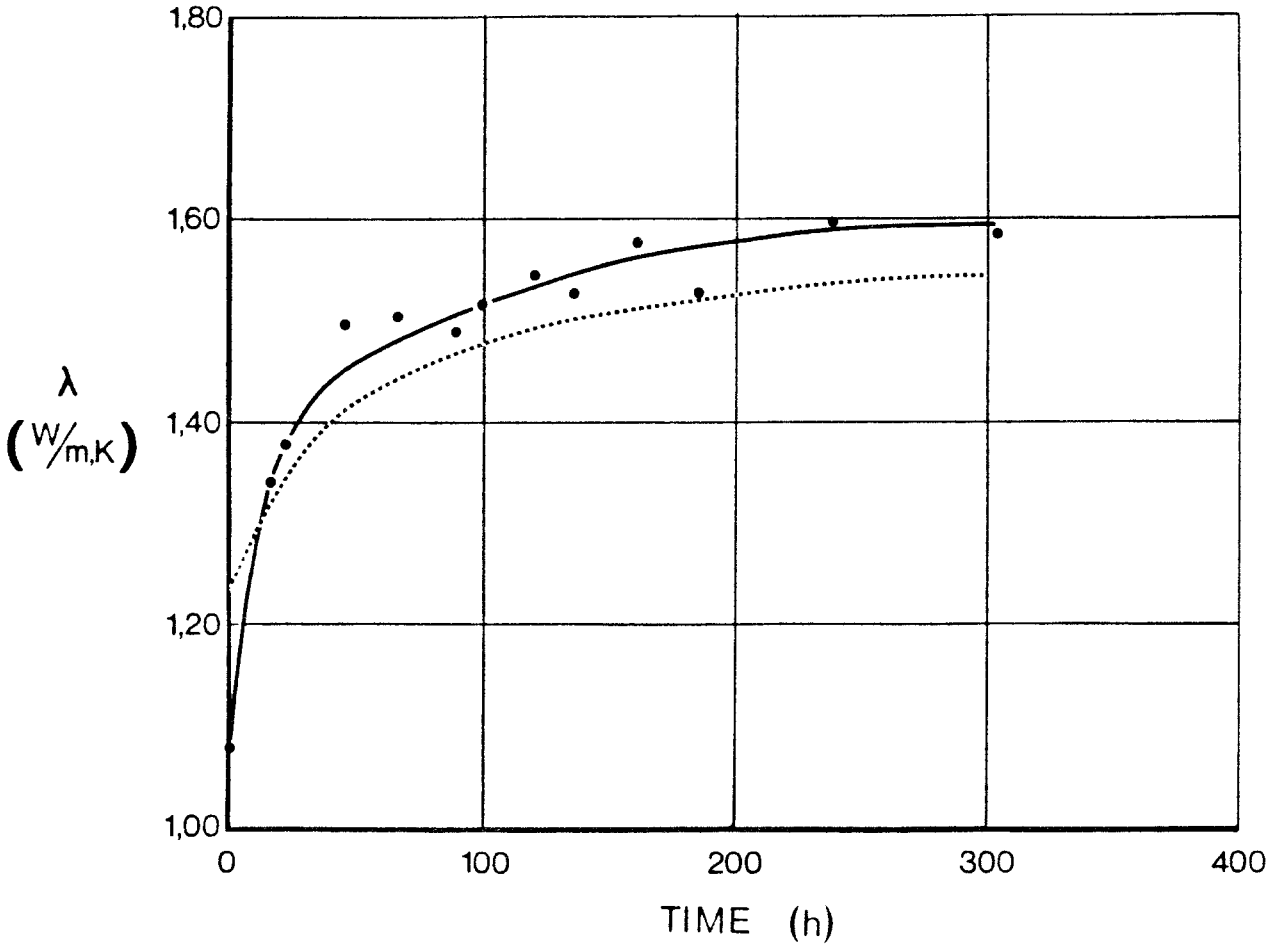

Fig. 4.4 The successive increase of the thermal conductivity of highly compacted bentonite as water is taken up. Water was subjected to the sample from the top side only. The broken line represents the calculated values.

For sample 4, the calculated water contents are shown in Table 3.

By the use of these values and eq. (14)-(17) the thermal conductivities at different times after the inlet of water could be calculated.

Table 3 Calculated water contents in the center of sample 4.

Time (hours)	Water content %
0	4,1
13,9	4,8
27,8	5,6
41,7	6,3
55,6	6,8
83,3	7,6
111,1	8,2
138,9	8,7
166,7	9,0
194,4	9,3
222,2	9,5
250,0	9,7

The results are shown in Fig. 4.4 and an acceptable resemblance is found between the calculated and recorded thermal conductivities.

Fig. 4.5 and 4.6 show the corresponding increase in thermal conductivity for the two samples 5 and 6 respectively.

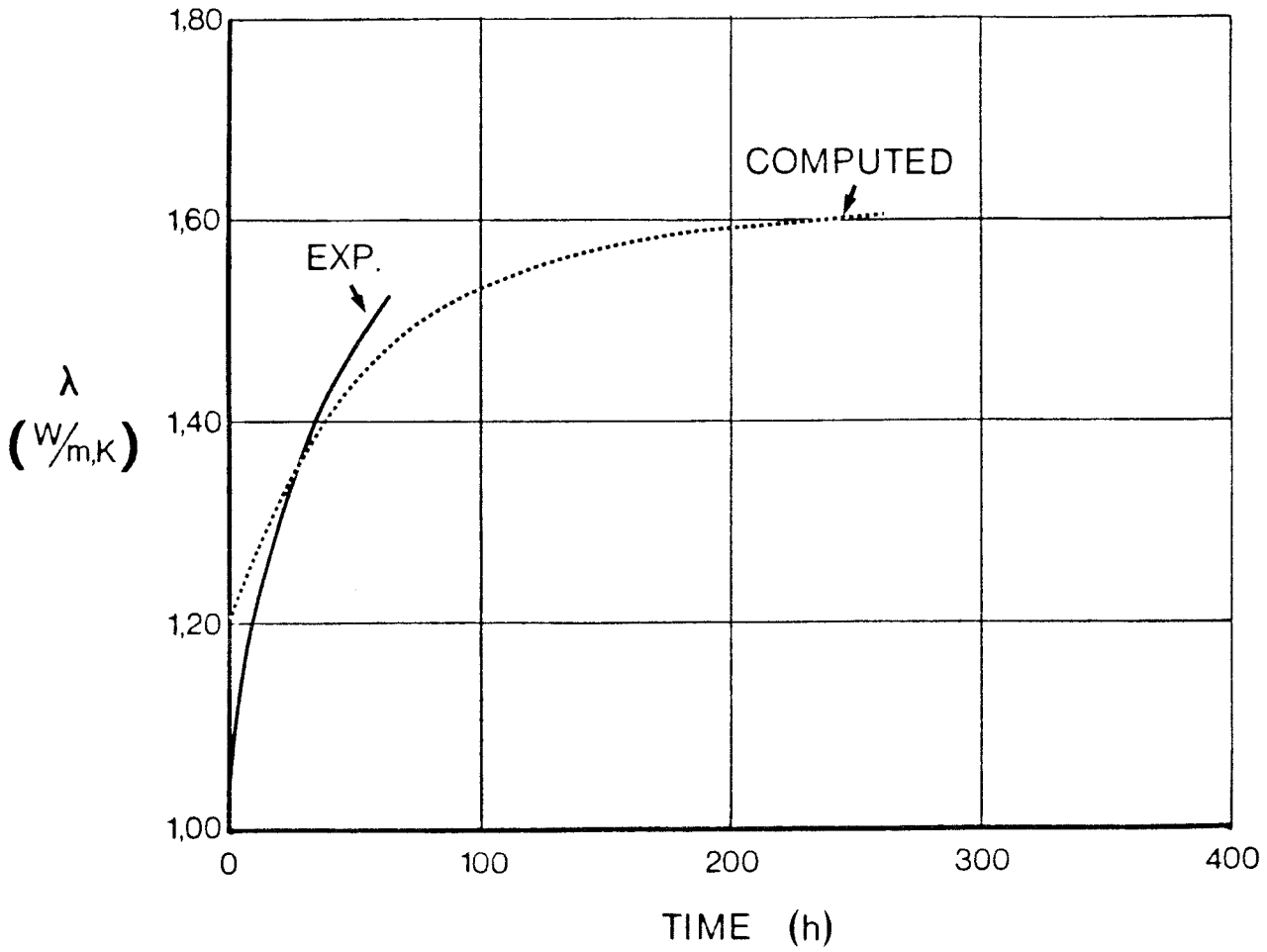

Fig. 4.5 The recorded and calculated increase of the thermal conductivity for sample 5. The bentonite was subjected to the water at time 0.

In sample 4 the swelling pressure and the conductivity were recorded simultaneously and Fig. 4.7 shows the relationship between the two parameters. As can be seen in Fig. 4.7 the conductivity increases with the swelling pressure, which is logical since the pressure increase is caused by the water uptake, which also increases the conductivity.

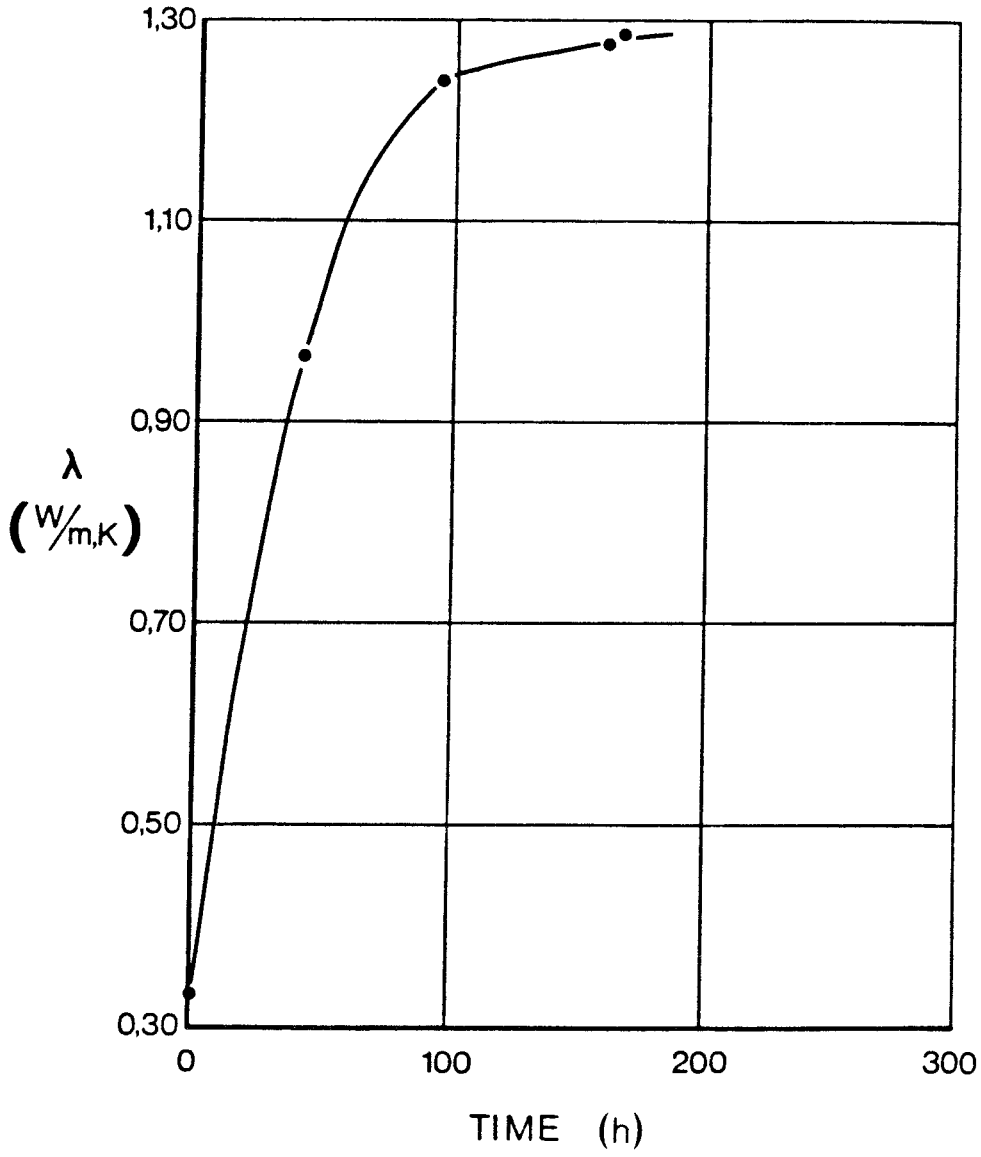

Fig. 4.6 The thermal conductivity as a function of time after water inlet in sample 6. This sample consisted of non-compacted powder bentonite.

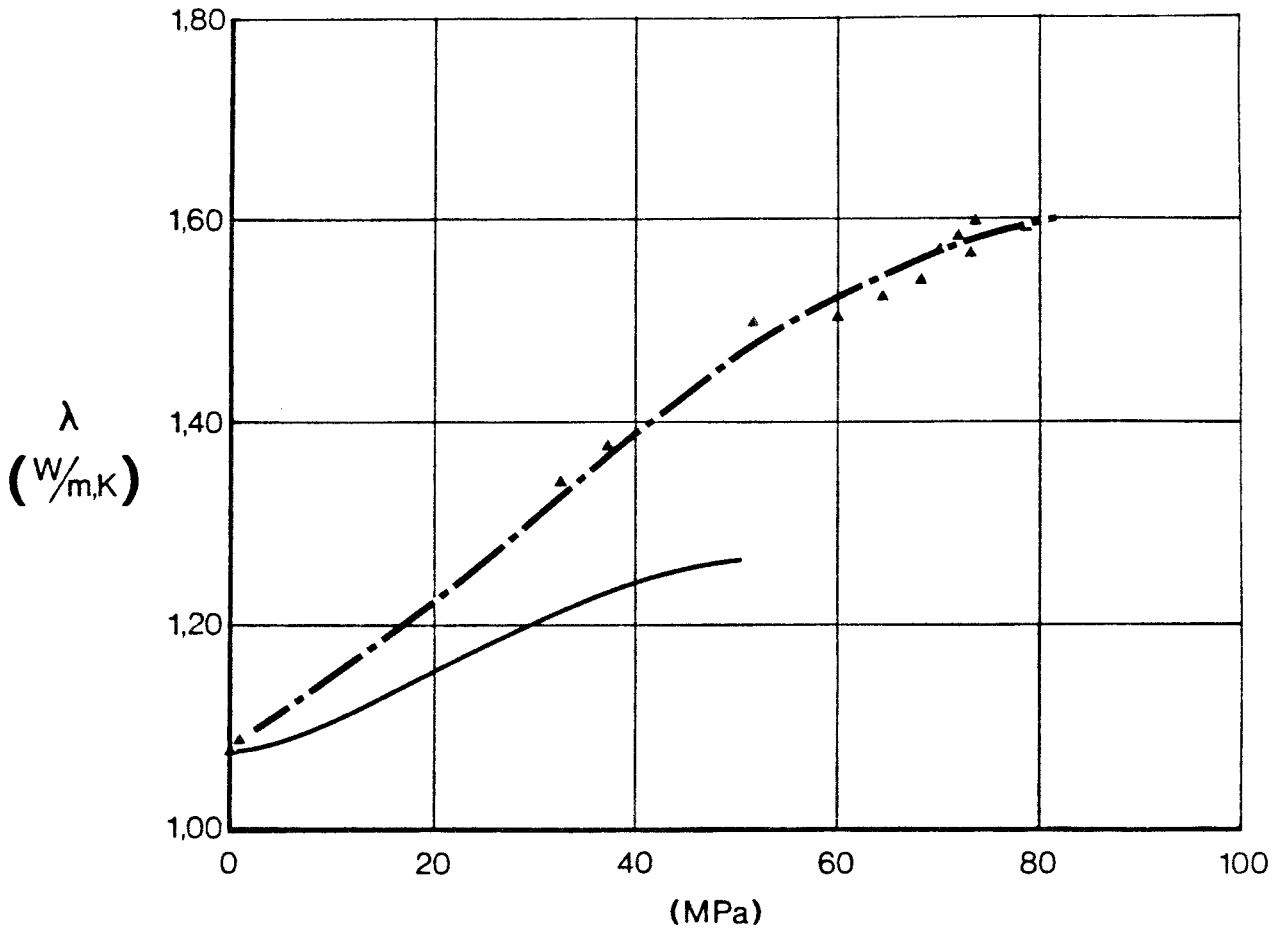

Fig. 4.7 The thermal conductivity as a function of the swelling pressure in sample 4. The solid line represents the pressure dependence of the "dry" sample, i.e. before water uptake.

If the increase of the conductivity due to pressure increase only, i.e. without any water uptake present, is taken into account it can be concluded that the conductivity in the swelling bentonite in this test was increased by 0,35 - 0,40 W/m,K due to water uptake.

Since the thermal diffusivity was determined at the same time as the thermal conductivity, it was possible also to determine the successive increase of the volumetric heat capacity as water was taken up by the bentonite.

Again, this was only possible for sample 4 for the reason given earlier.

Fig. 4.8 shows the volumetric heat capacity as a function of the time after water was let into the sample. As expected a successive increase was found as water was taken up. The heat capacity increased from $2,3 \cdot 10^6$ J/m^3,K for the "dry" sample to about $3,2 \cdot 10^6$ J/m^3,K at water saturation ($W_s \sim 10,2\%$).

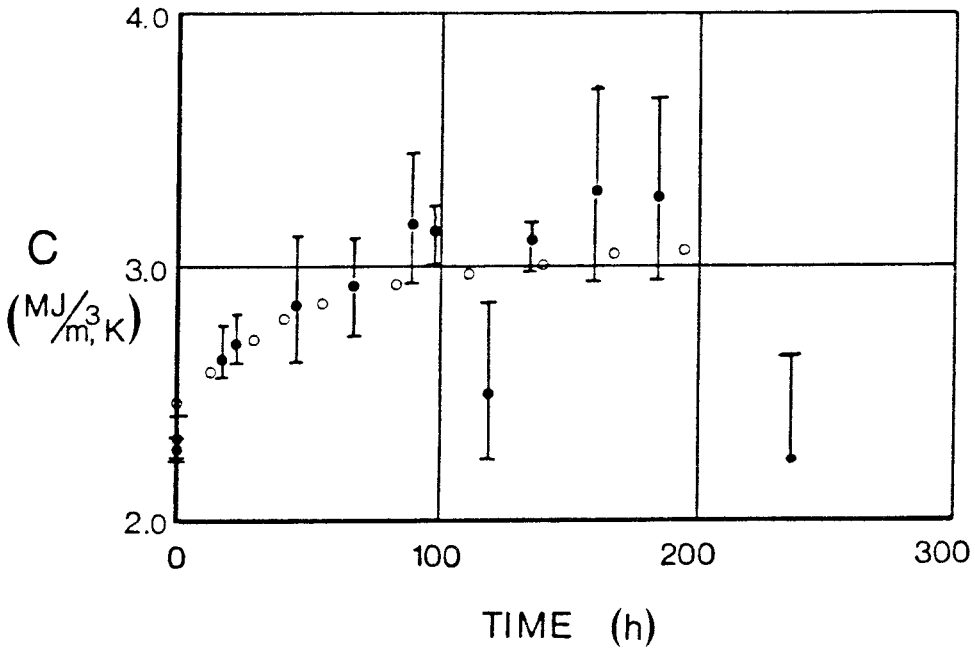

Fig. 4.8 The volumetric heat capacity as a function of the time after the water inlet into the oedometer. (●).
Calculated values are shown as well (O).

By using the same water contents as derived in Table 3 the theoretical increase of the heat capacity can be calculated by using eq. (18). These values are shown in Fig. 4.8 in addition. The calculations are based on a mean mass heat capacity of 1,05 J/g,K, which is

given by Fig. 4.3. There is a close resemblance between the recorded and calculated values before about 100 hours have passed. After this time the recorded values are higher, but the scatter increases as well. The latter can be explained by the experimental procedure, which is less accurate in the determination of the heat capacity than in the thermal conductivity. The high recorded values after about 100 hours are all connected with high coefficients of variations, typically above 10%. Taking this into account, the calculated values in all the cases lie within one σ-bound of each recorded value. However, at zero time, a discrepancy between the recorded and the calculated values still exists but this is explained by incomplete thermal contact between the metal strip and the bentonite. The relationship is clearly shown in Fig. 4.3. At zero external pressure the mass heat capacity is about 0,86 J/g,K giving a theoretical volumetric heat capacity of $2,15 \cdot 10^6$ J/m^3,K. This value should be compared to the somewhat larger recorded value of $2,26\text{-}2,31 \cdot 10^6$ J/m^3,K at the beginning of the actual test.

5. DISCUSSION

The thermal conductivity of highly compacted bentonite has been investigated as a function of the water content and the bulk density. This has been done by others, recently by Kahr et. al [4] and earlier by the author [6]. In the different investigations different testing methods were used. In [6] a radial stationary method was used giving a thermal conductivity of about 0,75 W/m,K for a sample characterized of ρ=2,02 t/m^3 and w=11%.

In the work by Kahr et. al [4]an instationary heating wire technique was used. The non-stationary method guaranteed, that no water redistribution due to thermal gradients took place during the test since the test is fast compared to the stationary heat flow methods.

A third method is used in this work. Here, a metal strip is place between two halves of the tested material. The strip is very small and can be placed in small volumes. This made it possible to mount the strip within a swelling pressure oedometer. The continuous change of the thermal conductivity as water was taken up could thus be detected. No water was redistributed during the test, since the measuring operation was finished within 10 seconds, and the two non-stationary methods should therefore yield comparable results.

From all the tests performed by Kahr et. al [4] an empirical relationship was derived giving the thermal conductivity of bentonite for different bulk densities, water contents and temperatures. Values obtained by this relationship have been compared to the experimental values presented in this report.

The theoretical model for the thermal conductivity given by eq. (14)-(17) and in [6], has also been used. This model was primarily derived for calculating the thermal conductivity of natural geological deposits. However, it has proved to be applicable to many soil materials and it is therefore reasonable to believe, that it also models the conductivity of the bentonite with reasonable accuracy.

In Fig. 5.1 all the experimentally obtained thermal conductivities from the present study have been plotted together with the theoretically deduced values. Both the described models were used.

From Fig. 5.1 it is clear that the model proposed by Kahr et. al [4] underestimates the thermal conductivity. This tendency is most pronounced for the constrained samples where they were subjected to large external pressures, samples 1-4. In the samples where the bentonite bodies were just kept together by a clamp with the metal strip in between, the calculated values were in closer accordance with the recorded values. The latter experimental procedure was similar to that used in [4] and it is therefore believed, that the increase of the recorded conductivity with increased pressure is due to an improved thermal contact between the strip and the surrounding sample. Consequently, when the pressure is low this contact is incomplete, leading to recorded values of the

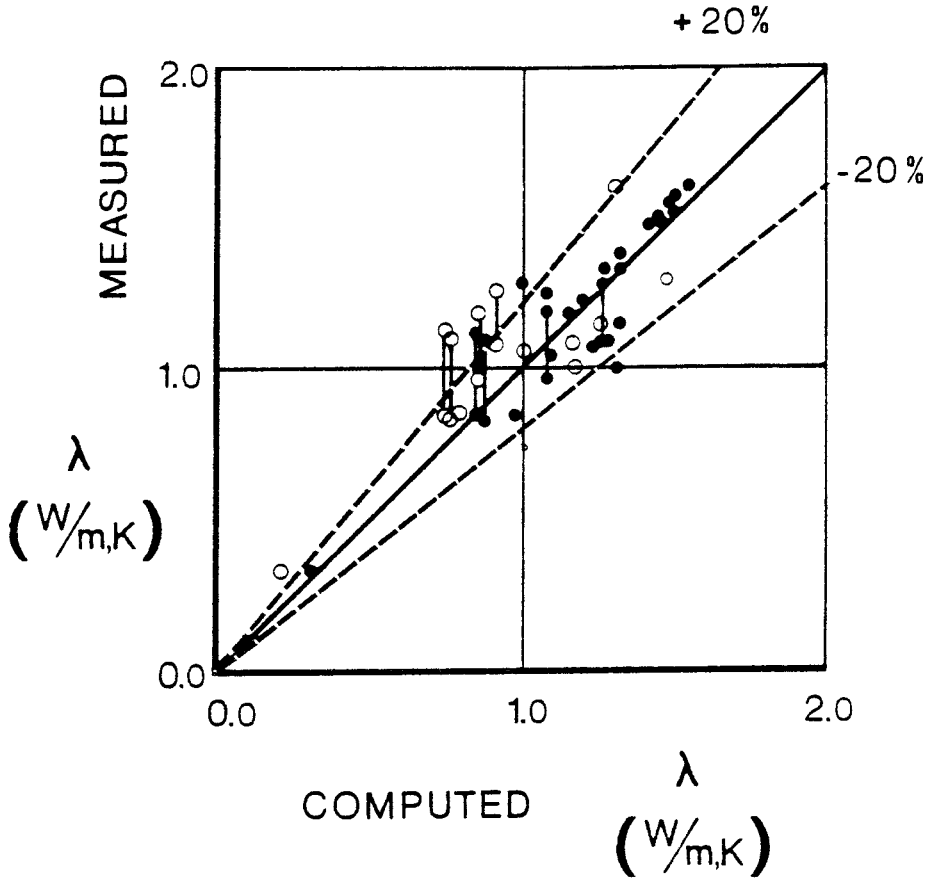

Fig. 5.1 Comparison between the experimentally obtained thermal conductivities and those calculated by the use of two different theoretical models.

- o represents values obtained by the model given in [4]
- ● represents values obtained by the model presented in this work eq. (14)-(17).

conductivities which are too small. Since the empirical model used in [4] is based on conductivities obtained from tests where the pressures on the samples have been low, it is logically explained that the model underestimates the values of constrained samples. The latter values are approximately 1.5 times higher than those yielded by the empirical relationship in [4].

The model presented here, eq. (14)-(17), and in [6] is in close agreement with the conductivities obtained from the constrained samples, but it slightly overestimates

the conductivities in the samples with low external pressure. The overestimation is due to incomplete contact between the metal strip and the sample. This means that the latter model, at present, seems to be the best one for calculating the conductivity in highly compacted bentonite. The model also gives a good agreement between the thermal conductivity and the time, when water is successively taken up by the bentonite, see Fig. 4.4.

It should be added here, that the influence of pressure on the resistivity of the metal strip has been determined as well. This was made by using data from a test on sample 1. In this test, the resistance in the metal strip, which was mounted in the oedometer, was determined at different pressures and temperatures. From the measured resistance it was then possible to compute the resistivity of the metal strip at different pressures. It was shown that the resistivity was practically insensitive for the pressures within the actual range, see Table 4. The determined resistivities were also close to the value which was used in the computations of the conductivities in the different tests, i.e. $\alpha=0.00348\ K^{-1}$.

Table 4. Computed resistivities of the metal strip

Pressure (MPa)	Resistivity (α) (K^{-1})
0	0.00360
10	0,00352
20	0,00349
30	0,00331
40	0,00339
50	0,00330

The experimental method used in [6] gave conductivities which were lower than those which could be computed by the use of eq. (14)-(17) and the equation given in [4]. The main reason for this is the incomplete thermal contact between the sample and the heating element in the center. However, the use of such an experimental procedure always yields conductivities which are lower than the "true" ones. In the application of the bentonite which is discussed here, i.e. as a buffer mass substance in a repository for nuclear waste, this will yield computed temperatures around a canister which are higher than those arising in a real repository. This means, that the conductivity obtained in this way will be on the "safe" side.

The thermal conductivities of highly compacted bentonite, which are discussed here, are all representative for conditions at room temperatures, i.e. about 20°C. At elevated temperatures the conductivity increases with the temperature and the dependency of this is given by eq. (19).

$$\lambda_{T_2} = \lambda_{T_1} [1+\beta(T_2-T_1)] \qquad (19)$$

where λ_{T_2} = thermal conductivity at the temperature T_2
λ_{T_1} = thermal conductivity at the temperature T_1
β = parameter for the temperature dependency

In Table 5 it is shown some data of the factor β in highly compacted bentonite for different temperature intervals. The value of this factor is in the range of $0.06 - 0.17 \cdot 10^{-2}$ $^{o}C^{-1}$, implying an increase of the conductivity with 3-8.5 percent if the temperature increases with 50 °C.

Table 5. The temperature correction factor for the thermal conductivity in compacted bentonite.

Material	Temperature (^{o}C)	β ($^{o}C^{-1}$)	Ref.
HCB Mx-80	58-43	$0.09\ 10^{-2}$	[6]
ρ=2.02 t/m^3	73-58	$0.17\ 10^{-2}$	[6]
w=11%	73-43	$0.14\ 10^{-2}$	[6]
HCB Mx-80	70-50	$0.06\ 10^{-2}$	[4]
ρ=2.0 t/m^3	90-70	$0.06\ 10^{-2}$	[4]
w=10%	90-50	$0.06\ 10^{-2}$	[4]

6 CONCLUSIONS

- The thermal conductivity of the highly compacted bentonite can at about +20 ^{o}C be computed by the use of eq. (14)-(17).

- Conductivities calculated by these equations are representative for bentonite bodies which have good thermal contact with its surroundings.

- The model is well describing the increase of the thermal conductivity as water is taken up.

- The volumetric heat capacity can be computed by eq. (18) as water is taken up.

- The mass heat capacity of the bentonite is, when the thermal contact is good, in the range of 0,96 - 1,05 J/g,K.
  If the thermal contact is incomplete, i.e. at low external pressures, the corresponding value is 0,80 - 0,87 J/g,K.

- By the use of the model described and the tests performed the thermal conductivity of the completely saturated bentonite with the bulk density of 2,0 - 2,1 t/m^3 can be estimated to 1,35 - 1,45 W/m,K. This is valid at room temperature (+20 ^{o}C).
  At higher temperatures the thermal conductivity will have a higher value; this increasing with about 0.1 percent per ^{o}C.

- The volumetric heat capacity for the saturated bentonite with the bulk density 2,0 - 2,1 t/m^3 can be computed to $3{,}10 \cdot 10^6$ - $3{,}40 \cdot 10^6$ J/m^3,K.

7. ACKNOWLEDGEMENTS

The author wishes to express his special thanks to Dr. Ernest Karawacki, Dept. of Physics, Chalmers University of Technology, who made possible the use of the electronic equipment involved in the THS-method. He was also responsible for some of the computer programs which were used in the present study.

Also, the author is very much indebted to Mr. Sven Juhlin and Mr. Lars Vikström, both at the Division of Soil Mechanics, University of Luleå, who were responsible for the experimental work and who made a very careful job.

8. REFERENCES

[1] Gustavsson, S.E. and Karawacki, E., 1979. Transient hot strip method for simultaneously measuring thermal conductivity and thermal diffusivity. Nordic Symposium on Earth Heat Pump Systems, pp. 55-61, Göteborg.

[2] Gustavsson, S.E., Karawacki, E. and Khan, M.N., 1979. Transient hot-strip method for simultaneously measuring thermal conductivity and thermal diffusivity of solids and fluids, J. Phys. D: Appl. Phys. vol. 12 pp. 1411-1421.

[3] Carslaw, H.S. and Jaeger, J.C., 1959. Conduction of heat in solids, Clarendon Press Oxford.

[4] Kahr, G. and Müller-von Moos, M., 1982. Wärmeleitfähigkeit von bentonit MX-80 und von Montigel nach der Heizdrahtmethode. Institut für Grundbau und Bodenmechanik, ETH, Zürich. Technischer Bericht 82-06, NAGRA, Baden.

[5] Pusch, R., 1980. Swelling pressure of highly compacted bentonite, Div. of soil mechanics, Luleå, KBS Technical Report TR 80-13.

[6] Knutsson, S., 1972. Värmeledningsförsök på buffertsubstans av kompakterad bentonit, Högskolan i Luleå, KBS Technical Report 72.

[7] Johansen, Ø. and Frivik, P.E., 1980. Thermal properties of soils and rock materials. The 2nd International Symposium on Ground Freezing, pp. 427-453, Norwegian Institute of Technology, Trondheim.

[8] Landolt-Börnstein, 1967. Jahlenwerte und Funktionen. IV. Band, 4. Teil Wärmetechnik, Bandteil. a. 975-944, Springer Verlag, Berlin.

[9] Pusch, R., Börgesson, L. and Nilsson, J., 1982. Buffer Mass Test - Buffer Materials. Stripa Project, Internal Report 82-06, Stockholm.

Appendix 1

Sample	$\bar{\lambda}$ (W/m,K)	$\bar{a}$ (10^{-7} m^2/s)	C (10^6 J/m^3,K)	C_s (J/g,K)	P (MPa)	S_λ (%)	S_a (%)
1	0,825	4,621	1,785	0,77	0	0,44	5,60
ρ=1,97 t/m^3	0,820	4,360	1,881	0,82	0	0,28	3,94
W_o=4,2%	0,889	4,184	2,125	0,95	10	0,90	5,50
	0,954	4,154	2,295	1,04	20	0,14	5,11
	1,012	4,418	2,290	1,04	30	0,89	1,25
	1,074	4,620	2,325	1,05	40	0,59	2,88
	1,102	4,728	2,330	1,06	50	0,88	2,02
2	0,843	4,111	2,051	0,91	0	0,28	5,04
ρ=1,96 t/m^3	0,916	3,926	2,333	1,06	10	0,17	1,44
W_o=4,2%	0,991	4,237	2,338	1,07	20	0,55	2,32
	1,044	4,446	2,348	1,07	30	0,68	2,54
	1,103	4,855	2,273	1,03	40	0,51	4,12
	1,128	4,647	2,428	1,11	50	0,08	1,74
3	0,962	4,945	1,945	0,80	0	0,40	1,35
ρ=2,09 t/m^3	1,014	4,627	2,191	0,92	10	0,43	4,18
W_o=4,2%	1,063	4,656	2,282	0,96	20	0,24	0,66
	1,118	4,850	2,306	0,98	30	0,33	2,45
	1,160	5,120	2,265	0,96	40	0,27	2,31
	1,184	4,957	2,388	1,02	50	0,68	2,57
4	1,083	4,782	2,264	0,914	0	0,38	1,82
ρ=2,17 t/m^3	1,105	4,307	2,566	1,059	10	0,58	3,23
W_o=4,1%	1,160	4,611	2,516	1,035	20	0,54	3,76
	1,199	4,776	2,509	1,032	30	0,38	0,72
	1,243	5,024	2,475	1,015	40	0,60	5,16
	1,265	5,155	2,453	1,005	50	0,57	4,46
	1,081	4,673	2,314	0,938	0	0,41	3,59

Appendix 2

Sample	Time (hours)	$\bar{\lambda}$ (W/m,K)	$\bar{a}$ (10^{-7} m^2/s)	C (10^6 J/m^3,K)	S_λ (%)	S_a (%)
4	16,5	1,343	5,065	2,650	0,42	3,96
ρ=2,17 t/m^3	20,8	1,378	5,085	2,711	0,35	3,71
W_o=4,1%	44,5	1,498	5,270	2,843	1,01	8,97
	65,7	1,505	5,229	2,878	1,19	6,83
	89,0	1,490	4,626	3,221	1,54	7,72
	98,0	1,517	4,885	3,106	0,30	1,21
	119,5	1,545	6,217	2,485	1,09	11,86
	136,0	1,523	5,009	3,050	0,26	2,40
	161,0	1,576	7,150	3,339	0,74	12,08
	185,0	1,527	4,636	3,294	1,50	11,30
	237,4	1,586	7,175	2,213	1,86	19,62
	304,1	1,586	12,690	1,250	0,77	14,06
5	0	0,833	4,161	2,002	0,80	6,53
ρ=2,01 t/m^3	14,5	1,044	4,481	2,107	0,52	3,09
W_o=5,3%	39,1	1,232	5,038	2,372	0,64	2,98
	63,2	1,325	4,980	2,715	1,36	9,05
6	0	0,331	2,331	1,420	1,67	4,66
ρ=1,158 t/m^3	43,1	0,970	4,513	2,149	1,33	3,39
W_o=10,1%	95,5	1,243	4,833	2,572	1,95	14,91
	161,8	1,281	4,729	2,709	0,13	3,42
	168,3	1,290	4,706	2,741	1,73	15,36

List of KBS's Technical Reports

1977–78
TR 121
KBS Technical Reports 1 – 120.
Summaries. Stockholm, May 1979.

1979
TR 79–28
The KBS Annual Report 1979.
KBS Technical Reports 79-01 – 79-27.
Summaries. Stockholm, March 1980.

1980
TR 80–26
The KBS Annual Report 1980.
KBS Technical Reports 80-01 – 80-25.
Summaries. Stockholm, March 1981.

1981
TR 81–17
The KBS Annual Report 1981.
KBS Technical Reports 81-01 – 81-16.
Summaries. Stockholm, April 1982.

TR 82–28
The KBS Annual Report 1982.
KBS Technical Reports 82-01 – 82-27.

1983
TR 83–01
Radionuclide transport in a single fissure A laboratory study
Trygve E Eriksen
Department of Nuclear Chemistry
The Royal Institute of Technology
Stockholm, Sweden 1983-01-19

TR 83–02
The possible effects of alfa and beta radiolysis on the matrix dissolution of spent nuclear fuel
I Grenthe
I Puigdomènech
J Bruno
Department of Inorganic Chemistry
Royal Institute of Technology
Stockholm, Sweden, January 1983

TR 83–03
Smectite alternation
Proceedings of a colloquium at State University of New York at Buffalo, May 26–27, 1982
Compiled by Duwayne M Anderson
State University of New York at Buffalo
February 15, 1983

TR 83–04
Stability of bentonite gels in crystalline rock – Physical aspects
Roland Pusch
Division Soil Mechanics, Univeristy of Luleå
Luleå, Sweden, 1983-02-20

TR 83–05
Studies in pitting corrosion on archeological bronzes – Copper
Åke Bresle
Jozef Saers
Birgit Arrhenius
Archaeological Research Laboratory
University of Stockholm
Stockholm, Sweden 1983-01-02

TR 83–06
Investigation of the stress corrosion cracking of pure copper
L A Benjamin
D Hardie
R N Parkins
University of Newcastle upon Tyne
Department of Metallurgy and engineering Materials
Newcastle upon Tyne, Great Britain, April 1983

TR 83–07
Sorption of radionuclides on geologic media – A literature survey.
I: Fission Products
K Andersson
B Allard
Department of Nuclear Chemistry
Chalmers University of Technology
Göteborg, Sweden 1983-01-31

TR 83–08
Formation and properties of actinide colloids
U Olofsson
B Allard
M Bengtsson
B Torstenfelt
K Andersson
Department of Nuclear Chemistry
Chalmers University of Technology
Göteborg, Sweden 1983-01-30

TR 83–09
Complexes of actinides with naturally occurring organic substances – Literature survey
U Olofsson
B Allard
Department of Nucluear Chemistry
Chalmers University of Technology
Göteborg, Sweden 1983-02-15

TR 83–10
Radilysis in nature: Evidence from the Oklo natural reactors
David B Curtis
Alexander J Gancarz
New Mexico, USA February 1983

TR 83–11
Description of recipient areas related to final storage of unreprocessed spent nuclear fuel
Björn Sundblad
Ulla Bergström
Studsvik Energiteknik AB
Nyköping, Sweden 1983-02-07

TR 83–12
Calculation of activity content and related propeties in PWR and BWR fuel using ORIGEN 2
Ove Edlund
Studsvik Energiteknik AB
Nyköping, Sweden 1983-03-07

TR 83–13
Sorption and diffusion studies of Cs and I in concrete
K Andersson
B Torstenfelt
B Allard
Department of Nuclear Chemistry
Chalmers University of Technology
Göteborg, Sweden 1983-01-15

TR 83–14
The complexation of Eu (III) by fulvic acid
J A Marinsky
State University of New York at Buffalo
Buffalo, NY 1983-03-31

TR 83–15
Diffusion measurements in crystalline rocks
Kristina Skagius
Ivars Neretnieks
Royal Institute of Technology
Stockholm, Sweden 1983-03-11

TR 83–16
Stability of deep-sited smectite minerals in crystalline rock – chemical aspects
Roland Pusch
Division of Soil Mechanics, University of Luleå
Luleå 1983-03-30

TR 83–17
Analysis of groundwater from deep boreholes in Gideå
Sif Laurent
Swedish Environmental Research Institute
Stockholm, Sweden 1983-03-09

TR 83–18
Migration experiments in Studsvik
O Landström
Studsvik Energiteknik AB
C-E Klockars
O Persson
E-L Tullborg
S Å Larson
Swedish Geological
K Andersson
B Allard
B Torstenfelt
Chalmers University of Technology
1983-01-31

TR 83–19
Analysis of groundwater from deep boreholes in Fjällveden
Sif Laurent
Swedish Environmental Research Institute
Stockholm, Sweden 1983-03-29

TR 83–20
Encapsulation and handling of spent nuclear fuel for final disposal
1 Welded copper canisters
2 Pressed copper canisters (HIPOW)
3 BWR Channels in Concrete
B Lönnerbeg, ASEA-ATOM
H Larker, ASEA
L Ageskog, VBB
May 1983

TR 83–21
An analysis of the conditions of gas migration from a low-level radioactive waste repository
C Braester
Israel Institute of Technology, Haifa, Israel
R Thunvik
Royal Institute of Technology
Stockholm, Sweden November 1982

TR 83–22
Calculated temperature field in and around a repository for spent nuclear fuel
Taivo Tarandi, VBB
Stockholm, Sweden April 1983

TR 83–23
Preparation of titanates and zeolites and their uses in radioactive waste management, particularly in the treatment of spent resins
Å Hultgren, editor
C Airola
Studsvik Energiteknik AB
S Forberg, Royal Institute of Technology
L Fälth, University of Lund
May 1983

TR 83–24
Corrosion resistance of a copper canister for spent nuclear fuel
The Swedish Corrosion Research Institute
and its reference group
Stockholm, Sweden April 1983

TR 83–25
Feasibility study of electron beam welding of spent nuclear fuel canisters
A Sanderson, T F Szluha, J L Turner, R H Leggatt
The Welding Institute Cambridge
The United Kingdom April 1983

TR 83–26
The KBS UO_2 leaching program
Summary Report 1983-02-01
Ronald Forsyth, Studsvik Energiteknik AB
Nyköping, Sweden February 1983

TR 83–27
Radiation effects on the chemical environment in a radioactive waste repository
Trygve Eriksen
Royal Institute of Technology, Stockholm
Arvid Jacobsson
Univerisity of Luleå
Luleå, Sweden 1983-07-01

TR 83–28
An analysis of selected parameters for the BIOPATH-program
U Bergström
A-B Wilkens
Studsvik Energiteknik AB
Nyköping, Sweden 1983-06-08

TR 83–29
On the environmental impact of a repository for spent nuclear fuel
Otto Brotzen
Stockholm, Sweden april 1983

TR 83–30
Encapsulation of spent nucler fuel – Safety Analysis
ES-konsult AB
Stockholm, Sweden April 1983

TR 83–31
Final disposal of spent nuclear fuel – Standard programme for site investigations
Compiled by
Ulf Thoregren
Swedish Geological
April 1983

TR 83–32
Feasibility study of detection of defects in thick welded copper
Tekniska Röntgencentralen AB
Stockholm, Sweden April 1983

TR 83–33
The interaction of bentonite and glass with aqueous media
M Mosslehi
A Lambrosa
J A Marinsky
State University of New York
Buffalo, NY, USA April 1983

TR 83–34
Radionuclide diffusion and mobilities in compacted bentonite
B Torstenfelt
B Allard
K Andersson
H Kipatsi
L Eliasson
U Olofsson
H Persson
Chalmers University of Technology
Göteborg, Sweden April 1983

TR 83–35
Actinide solution equilibria and solubilities in geologic systems
B Allard
Chalmers University of Technology
Göteborg, Sweden 1983-04-10

TR 83–36
Iron content and reducing capacity of granites and bentonite
B Torstenfelt
B Allard
W Johansson
T Ittner
Chalmers University of Technology
Göteborg, Sweden April 1983

TR 83–37
Surface migration in sorption processes
A Rasmuson
I Neretnieks
Royal Institute of Technology
Stockholm, Sweden March 1983

TR 83–38
Evaluation of some tracer tests in the granitic rock at Finnsjön
L Moreno
I Neretnieks
Royal Institute of Technology, Stockholm
C-E Klockars
Swedish Geological
Uppsala April 1983

TR 83–39
Diffusion in the matrix of granitic rock Field test in the Stripa mine. Part 2
L Birgersson
I Neretnieks
Royal Institute of Technology
Stockholm, Sweden March 1983

TR 83–40
Redox conditions in groundwaters from Svartboberget, Gideå, Fjällveden and Kamlunge
P Wikberg
I Grenthe
K Axelsen
Royal Institute of Technology
Stockholm, Sweden 1983-05-10

TR 83–41
Analysis of groundwater from deep boreholes in Svartboberget
Sif Laurent
Swedish Environmental Research Institute
Stockholm, Sweden 1983-06-10

TR 83–42
Final disposal of high-levels waste and spent nuclear fuel – foreign activities
R Gelin
Studsvik Energiteknik AB
Nyköping, Sweden May 1983

TR 83–43
Final disposal of spent nuclear fuel – geological, hydrogeological and geophysical methods for site characterization
K Ahlbom
L Carlsson
O Olsson
Swedish Geological
Sweden May 1983

TR 83–44
Final disposal of spent nuclear fuel – equipment for site characterization
K Almén, K Hansson, B-E Johansson, G Nilsson
Swedish Geological
O Andersson, IPA-Konsult
P Wikberg, Royal Institute of Technology
H Åhagen, SKBF/KBS
May 1983

TR 83–45
Model calculations of the groundwater flow at Finnsjön, Fjällveden, Gideå and Kamlunge
L Carlsson
A Winberg
Swedish Geological, Göteborg
B Grundfelt
Kemakta Consultant Company,
Stockholm May 1983

TR 83–46
Use of clays as buffers in radioactive repositories
Roland Pusch
University of Luleå
Luleå May 25 1983

TR 83–47
Stress/strain/time properties of highly compacted bentonite
Roland Pusch
University of Luleå
Luleå May 1983

TR 83–48
Model calculations of the migration of radio-nuclides from a respository for spent nuclear fuel
A Bengtsson
Kemakta Consultant Company, Stockholm
M Magnusson
I Neretnieks
A Rasmuson
Royal Institute of Technology, Stockholm
May 1983

TR 83–49
Dose and dose commitment calculations from groundwaterborne radioactive elements released from a repository for spent nuclear fuel
U Bergström
Studsvik Energiteknik AB
Nyköping, Sweden May 1983

TR 83–50
Calculation of fluxes through a repository caused by a local well
R Thunvik
Royal Institute of Technology
Stockholm, Sweden May 1983

TR 83–51
GWHRT – A finite element solution to the coupled ground water flow and heat transport problem in three dimensions
B Grundfelt
Kemakta Consultant Company
Stockholm, Sweden May 1983

TR 83–52
Evaluation of the geological, geophysical and hydrogeological conditions at Fjällveden
K Ahlbom
L Carlsson
L-E Carlsten
O Duran
N-Å Larsson
O Olsson
Swedish Geological
May 1983

TR 83–53
Evaluation of the geological, geophysical and hydrogeological conditions at Gideå
K Ahlbom
B Albino
L Carlsson
G Nilsson
O Olsson
L Stenberg
H Timje
Swedish Geological
May 1983

TR 83–54
Evaluation of the geological, geophysical and hydrogeological conditions at Kamlunge
K Ahlbom
B Albino
L Carlsson
J Danielsson
G Nilsson
O Olsson
S Sehlstedt
V Stejskal
L Stenberg
Swedish Geological
May 1983

TR 83–55
Evaluation of the geological, geophysical and hydrogeological conditions at Svartboberget
K Ahlbom
L Carlsson
B Gentzschein
A Jämtlid
O Olsson
S Tirén
Swedish Geological
May 1983

TR 83–56
I: Evaluation of the hydrogeological conditions at Finnsjön
L Carlsson
G Gidlund
II: Supplementary geophysical investigations of the Stärnö peninsula
B Hesselström
Swedish Geological
May 1983

TR 83–57
Neotectonics in northern Sweden – geophysical investigations
H Henkel
K Hult
L Eriksson
Geological Survey of Sweden
L Johansson
Swedish Geological
May 1983

TR 83–58
Neotectonics in northern Sweden – geological investigations
R Lagerbäck
F Witschard
Geological Survey of Sweden
May 1983

TR 83–59
Chemistry of deep groundwaters from granitic bedrock
B Allard
Chalmers University of Technology
S Å Larson
E-L Tullborg
Swedish Geological
P Wikberg
Royal Institute of Technology
May 1983

TR 83–60
On the solubility of technetium in geochemical systems
B Allard
B Torstenfelt
Chalmers University of Technology
Göteborg, Sweden 1983-05-05

TR 83–61
Sorption behaviour of well-defined oxidation states
B Allard
U Olofsson
B Torstenfelt
H Kipatsi
Chalmers University of Technology
Göteborg, Sweden 1983-05-15

TR 83–62
The distribution coefficient concept and aspects on experimental distribution studies
B Allard
K Andersson
B Torstenfelt
Chalmers University of Technology
Göteborg, Sweden May 1983

TR 83–63
Sorption of radionuclides in geologic systems
K Andersson
B Torstenfelt
B Allard
Chalmers University of Technology
Göteborg, Sweden 1983-06-15

TR 83–64
Ion exchange capacities and surface areas of some major components and common fracture filling materials of igneous rocks
B Allard
M Karlsson
Chalmers University of Technology
E-L Tullborg
S Å Larson
Swedish Geological
Göteborg, Sweden May 1983

TR 83–65
Sorption of actinides on uranium dioxide and zirconium dioxide in connection with leaching of uranium dioxide fuel
B Allard
N Berner
K Andersson
U Olofsson
B Torstenfelt
Chalmars University of Technology
R Forsyth
Studsvik Energiteknik AB
May 1983

TR 83–66
The movement of radionuclides past a redox front
I Neretnieks
B Åslund
Royal Institute of Technology
Stockholm, Sweden 1983-04-22

TR 83–67
Some notes in connection with the studies of final disposal of spent fuel. Part 2
I Neretnieks
Royal Institute of Technology
Stockholm, Sweden May 1983

TR 83–68
Two dimensional movements of a redox front downstream from a repository for nuclear waste
I Neretnieks
B Åslund
Royal Institute of Technology
Stockholm, Sweden 1983-06-03

TR 83–69
An approach to modelling radionuclide migration in a medium with strongly varying velocity and block sizes along the flow path
I Neretnieks
A Rasmuson
Royal Institute of Technology
Stockholm, Sweden May 1983

TR 83–70
Analysis of groundwater from deep boreholes in Kamlunge
S Laurent
Swedish Environmental Research Institute
Stockholm, Sweden May 1983

TR 83–71
Gas migration through bentonite clay
Roland Pusch
Thomas Forsberg
University of Luleå
Luleå, Sweden May 31, 1983

TR 83–72
On the thermal conductivity and thermal diffusivity of highly compacted bentonite
Sven Knutsson
University of Luleå
Luleå, Sweden October 1983